MICRODROPLETS IN HIGH TEMPERATURE GRADIENTS GENERATING POROUS CATALYTIC MICROBEADS

Corentin Tregouet[1,2,*], Johan Bomer[1], Mathieu Odijk[1], Detlef Lohse[2], Albert van den Berg[1]

[1]BIOS-Lab-on-a-Chip group, MESA+, MIRA, Max Planck Center for Complex Fluid dynamics, University of Twente, the Netherlands

[2]Physics of Fluids group, MESA+, MIRA, Max Planck Center for Complex Fluid dynamics, University of Twente, the Netherlands

ABSTRACT

A renewable production of hydrogen would enable the further development of carbon-dioxide emission-free vehicles. Ethanol reforming is a very promising lead which necessitates nanocatalysts. We propose here a method to embed nanocatalysts in porous microbeads and thus facilitates their use. We developed a microfluidic chip enabling a sharp temperature gradient to generate in-drop phase separation and template porous microbeads. Using this chip, we produce microbeads of around 50 µm diameter, with pores of the order of 1 µm in which nanoparticles are embedded.

KEYWORDS: Microfluidics, Phase Separation, Porous Material, Droplets, Catalysis.

INTRODUCTION

Hydrogen is one of the most promising sources of energy for vehicles in the future. Even if its conversion in energy produces only water, we have no environment-friendly method to produce enough hydrogen to supply the energy market yet. However, hydrogen can be produced from water and ethanol through solar energy with the use of heterogeneous catalysts [1]. This reaction of ethanol reforming is more efficient with nanocatalysts since they present a high surface/volume ratio [2], and thus a high activity for a low amount of material. The draw-back of these nanocatalyst is the difficulty to handle and recover them. For this reason they are usually embedded in porous substrates [3,4].

Our aim is to develop a versatile matrix, with controlled porosity, into which various types of nanocatalyst can be embedded, and which can be used in different types of reactors. Moreover, to ensure the efficiency of the catalyst, a large contact area between the nanocatalyst and the reaction media is required, such as efficient transport of the reactants and products through the matrix. It has been shown that an optimal support to that end should exhibit a hierarchy of different pore sizes [5]. By producing solidified biphasic droplets in microfluidic devices as presented in Figure 1, we will combine the multiscale porosity of these materials with the precise control of the microparticles' shape enabled by microfluidics. In this approach, the nanocatalysts adsorb at the interface during the pore formation.

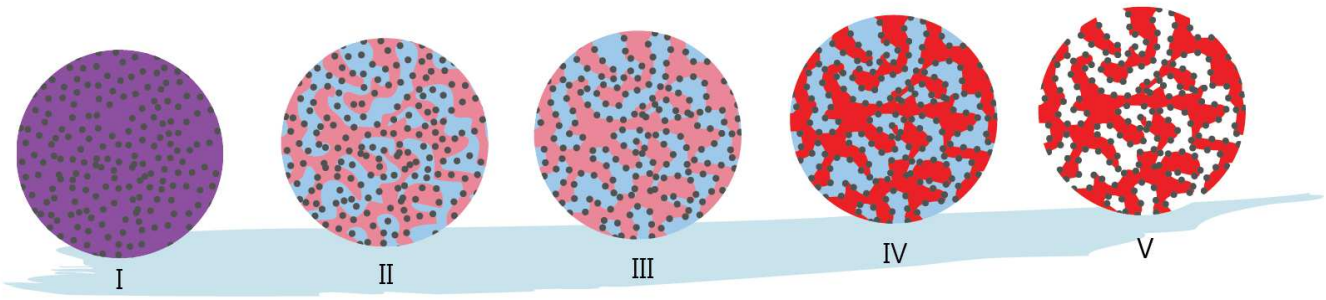

Figure 1: five steps of particle production. I: homogeneous droplet loaded with nanocatalysts; II: demixing; III: nanoparticle trapping at the interface; IV: photo-polymerization of phase A (red); V: rinsing of phase B (blue).

In this work we present a method and a microfluidic chip to prepare porous microbeads embedding nanocatalysts. Our approach is based on the demixing of a polymer-mixture inside micrometric droplets triggered by a temperature drop and solidify with UV, as presented in Figure 1. Finally, the second phase is dissolved in ethanol

to obtain a porous microsphere. A good control of the demixing and the polymerization is needed to have a well-defined porosity and reproducibility. This requires precise control of temperature and time achievable with microfluidics [6-8].

EXPERIMENTAL

A microfluidic chip has been designed and fabricated to produce droplets of polymer in oil at high temperature. The droplets are then conveyed along a channel through a temperature gradient to quickly cool them down and trigger their phase separation.

The microfluidic chip consists of a first wafer of borosilicate glass on which platinum is deposited using lithography for the electrodes and a heat sink, and then covered with 1µm of silicon dioxide by PECVD (plasma-enhanced chemical vapor deposition) everywhere except on top of the connecting pads. This wafer is bonded at 600 °C (direct bonding) to a second borosilicate wafer in which semicircular 300 µm-wide channels are etched using HF.

The temperature gradient is set with heating electrodes controlled with in-situ platinum temperature probes, and a heat sink to dissipate heat in the cold zone of the chip, as shown in Figures 2a and 2b. On-chip temperature probes consist of platinum resistors whose resistances depend on temperature. A Peltier element can be put in contact with the cold zone of the chip to increase the temperature gradient.

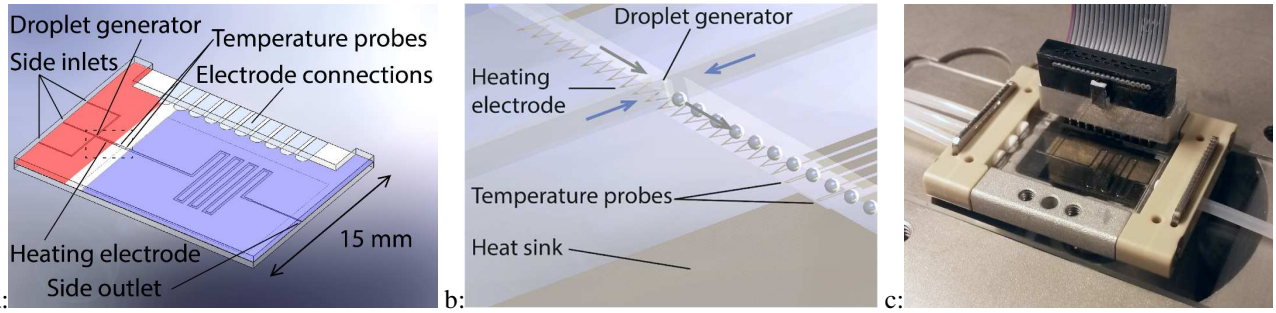

Figure 2: a: schematic of the glass microfluidic chip for particles production with the hot area (red) and the cool area (blue). b: close-up on the framed area. The probes are separated by 500 µm; c: microfluidic chip in the chip holder connected to the temperature regulator and the flow-rate controller.

The chip is connected to a computer thanks to a chip holder adapted from a commercially-available one (Figure 2c) to measure and adjust the hot temperature, and the cold temperature when a Peltier element is used. Finite-element simulations have been performed using Comsol Multiphysics to predict the temperature inside the chip and estimate the necessary heating voltage.

Droplets consist of a mixture of poly(ethylene glycol) diacrylate (PEGDA) and poly(propylene glycol) (PPG) at a mass ratio of 0.47/0.53. Nanoparticles of titania (20 nm) and a photo-initiator (Darocur 1173) are also added to the mixture.

The phase separation of these polymers is known to be relatively slow (about 1 s [9]), and the solidification to be fast (about 0.2 s [10]). In this specific proportion of polymers, phase separation occurs at a critical temperature of 55°C, and yields a bi-continuous structure (spinodal decomposition). By photocuring the PEGDA phase and rinsing the PPG, we can therefore synthesize porous microbeads loaded with model titania nanoparticles or nano-catalysts.

The alignment of the temperature gradient with the UV beam is our parameter of control to tune the properties of our system of pores: the more length we let between the temperature drop and the UV solidification, the more time the droplets will have to experience phase separation before being solidified. The width of the pores can therefore be adjusted by controlling the relative position of the temperature gradient and of the UV-beam.

RESULTS AND DISCUSSION

Simulations on Figure 3 show a peak of temperature at the droplet generator due to the convergence of the channels and thus of the heaters. Just after this peak a sharp gradient temperature is observed. The gradient is maximum between the end of the heater and the beginning of the heat sink due to the poor thermal conductivity of

this area, and we find that by supplying the heaters with a voltage of 26 V the point where temperature is equal to 55 °C is located between our two temperature probes.

Experimentally, a temperature gradient of 25 K/mm is measured between our temperature probes (separated by 500 µm). Using the Peltier element, a gradient of 40 K/mm can be achieved. Compared to the simulations, we need a slightly higher voltage to have similar temperatures (30 V), but the measured gradient is greater than in the simulations. We think that this is due to the network of electrodes connected to the temperature probes acting as a supplementary heat-sink, which is not taken into account in our simulations. In reality, the space between the heaters and the temperature probes is partially covered by platinum electrodes, which should prevent the high gradient that we observe in our simulation upstream of our temperature probes. However this high gradient allows a precise knowledge of the moment (and position) where the phase separation starts, which is of great importance to synchronize phase separation and solidification.

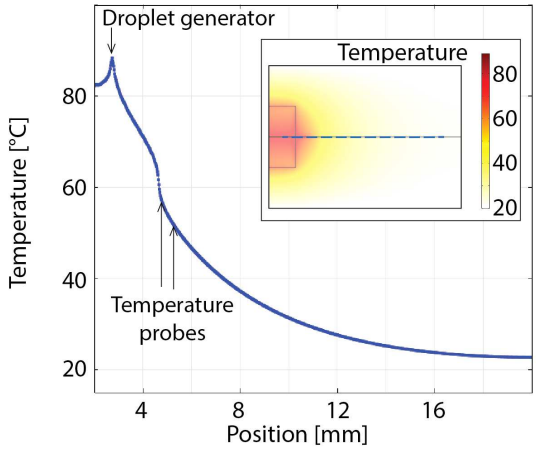

Figure 3: simulated temperature profile along the dotted line, aligned with the main channel. This simulation was realized for a heating voltage of 26 V, which is what we also use in our experiments.

Using this chip, droplets of about 50 µm diameter are formed and solidified to beads such as the one presented in Figure 4a. After rinsing with ethanol, the porous structure becomes visible (Figure 4b-c). The pores can be observed with scanning electron microscopy, and their typical size is 1 µm as visible in Figure 4c.

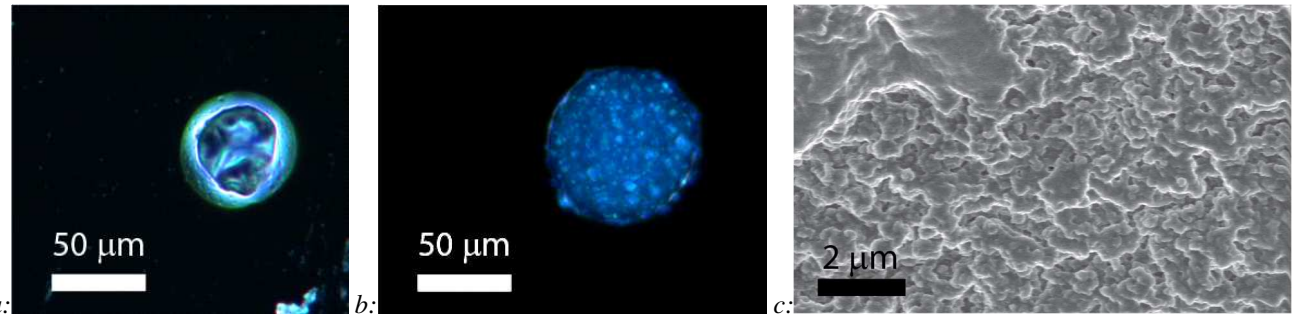

Figure 4: a:particle obtained before rinsing with ethanol (dark field) b: aspect of a particle after rinsing with ethanol dark field); c: scanning Electron Microscopy image of the surface of a particle after rinsing with ethanol. (Courtesy of H. Le The and MESA+).

In the near future, we will use this method with nanocatalyst instead of the model titania nanoparticles. Moreover, we want to characterize more precisely the porous structure of our beads. Finally, we will measure the catalytic activity of our beads and optimize it by adjusting the size of the pores that depends on the alignment of the UV beam with the temperature gradient.

CONCLUSION

We developed a chip that allows us to produce droplets at high temperature and to quickly cool them down to trigger a phase separation inside these droplets. The combination of in-situ platinum electrodes and platinum heat-sink allows a temperature gradient of 25 K/mm which reaches 40 K/mm when the heat-sink is coupled with a Peltier element. Using photo-curable polymers, we produce porous microbeads with pores smaller than 1 µm in which nanoparticle or nanocatalyst are embedded. This will facilitate the use of various nanocatalysts which are developed to catalyze ethanol reforming and thus hydrogen production.

ACKNOWLEDGEMENTS

This work was supported by the Netherlands Center for Multiscale Catalytic Energy Conversion (MCEC), and the Netherlands Organisation for Scientific Research (NWO) Gravitation program funded by the Ministry of Education, Culture and Science of the government of the Netherlands.

REFERENCES

[1] F. Li, Q. Gu, Y. Niu, R. Wang, Y. Tong, S. Zhu, H. Zhang, Z. Zhang, X. Wang, *Appl. Surf. Sci.*, **391**, 251–258, (2017).

[2] M. Cargnello, T. Montini, S. Y. Smolin, J. B. Priebe, J. J. Delgado Jaén, V. V. T. Doan-Nguyen, I. S. McKay, J. A. Schwalbe, M.-M. Pohl, T. R. Gordon, Y. Lu, J. B. Baxter, A. Brückner, P. Fornasiero, C. B. Murray, *Proc. Natl. Acad. Sci.*, **113** (15), 3966–3971, (2016).

[3] I. K. Sung, C. M. Mitchell, D. P. Kim, P. J. A. Kenis, *Adv. Funct. Mater.*, **15** (8), 1336–1342, (2005).

[4] E. Shirman, T. Shirman, A. V. Shneidman, A. Grinthal, K. R. Phillips, H. Whelan, E. Bulger, M. Abramovitch, J. Patil, R. Nevarez, J. Aizenberg, *Adv. Funct. Mater.*, **28**, (2017).

[5] E. T. C. Vogt, B. M. Weckhuysen, *Chem. Soc. Rev.* **44**, 7342–7370 (2015).

[6] Y. Liu and X. Jiang, *Lab Chip*, **17** (23), 3960–3978, (2017).

[7] R. Seemann, M. Brinkmann, T. Pfohl, S. Herminghaus, S., *Rep. Prog. Phys*. **75,** 16601–41 (2012).

[8] B. Shen, J. Ricouvier, F. Malloggi, P. Tabeling, *Adv. Sci*. **3,** 1600012 (2016).

[9] M. N. Lee, A. Mohraz. *Adv. Mat.,* **22** (43), 4836–4841, (2010).

[10] G. C. Le Goff, J. Lee, A. Gupta, W. A. Hill, P. S. Doyle. *Adv. Sci.*, **2** (10), 1500149, (2015).

CONTACT

* C.B.M. Tregouet; phone: +31-53-489-4476; c.b.m.tregouet@utwente.nl